KSME

Springer

Journal of Mechanical Science and Technology 38 (6) 2024

Original Article
DOI 10.1007/s12206-024-2204-4

Keywords:
· Journal bearing
· Linear
· Nonlinear
· Rigid rotor
· Wear

Correspondence to:
Jawaid Iqbal Inayat-Hussain
jawaid@uniten.edu.my

Citation:
Moorthi, L. R., Inayat-Hussain, J. I., Zakaria, A. A. (2024). Effect of bearing wear on linear and nonlinear responses of a rigid rotor supported by journal bearings. Journal of Mechanical Science and Technology 38 (6) (2024) 2741~2747. http://doi.org/10.1007/s12206-024-2204-4

Received January 9th, 2024
Revised February 14th, 2024
Accepted February 19th, 2024

† This paper was presented at International Session in KSME Annual Meeting 2023, Songdo Convensia, Incheon, Korea & Online, November 1-4, 2023. Recommended by Guest Editor Gunwoo Noh

© The Korean Society of Mechanical Engineers and Springer-Verlag GmbH Germany, part of Springer Nature 2024

# Effect of bearing wear on linear and nonlinear responses of a rigid rotor supported by journal bearings

**Logamurthi Raja Moorthi[1,2], Jawaid Iqbal Inayat-Hussain[3,4] and Azrul Abidin Zakaria[3,4]**

[1]College of Graduate Studies, Universiti Tenaga Nasional, Kajang, Selangor, Malaysia, [2]Tenaga Nasional Berhad, Kuala Lumpur, Malaysia, [3]College of Engineering, Universiti Tenaga Nasional, Kajang, Selangor, Malaysia, [4]Institute of Power Engineering, Universiti Tenaga Nasional, Kajang, Selangor, Malaysia

**Abstract** Linearized dynamic bearing coefficients are commonly used to determine the vibration response of rotors supported by journal bearings. Journal bearings can, however, behave nonlinearly, particularly in the presence of bearing wear. This work was undertaken to examine the effect of bearing wear severity on the linear and nonlinear responses of a rigid rotor at low, moderately, and highly loaded operating regime. Numerical results showed that the center of the nonlinear orbit coincides with the center of the linear orbit for all three operating regimes in non-worn bearing. However, in worn bearings, the center of the nonlinear orbit shifts away from the center of the linear orbit for all three operating regimes. The nonlinear analysis also showed that super-synchronous vibration response may occur, particularly at highly loaded operating regimes and at the maximum wear depth investigated in this work.

## 1. Introduction

Journal bearings play an important role in the dynamics of rotating machines and are widely utilized in industry. However, these bearings are exposed to a gradual wear development amidst the rotating machine's operation, particularly during starts and stops or when passing through the rotor's critical speed [1]. As such, the bearing's geometry gets altered, thereby altering its dynamic characteristics, and inducing vibrations, which may lead to destructive failures [2]. Wear is amongst the most frequent failure that affects the bearing clearance at first hand and causes alterations to the rotating machine dynamics [3]. In the presence of wear, the pressure distribution, the rotor's equilibrium position, the bearing's dynamic coefficients and the system's response changes due to the alteration in oil film thickness [4].

For the computation of the vibration response of rotors in journal bearings, linearized dynamic coefficients are widely utilized. Lund et al. [5, 6] established a technique to linearize the bearing forces to obtain the stiffness and damping coefficients by infinitesimal perturbations. Despite these coefficients being mathematically accepted for infinitesimal amplitudes, the author stated that, in practice, they would be consistent for journal movements up to 40 % of the radial clearance. In the same articles, discrepancies between linear and nonlinear orbits were observed, nevertheless it was asserted that they were still in accord. Thenceforth, the investigation of linear coefficients behavior and their representativeness in the dynamic response of rotating machines expanded, becoming the popular method for illustrating how the journal bearings affect the behavior of rotating systems [7, 8]. Although adopting linear stiffness and damping coefficients for bearings are more convenient, these bearings occasionally exhibit nonlinear behavior that affects the response of the rotating machines, as has been reported by Viana et al. [7] and Machado et al. [8]. Rotor-bearing systems have been observed to exhibit sub- and super-synchronous responses, chaos and thermally induced instability due to nonlinearity in the journal bearings and the structures that surround them [9]. Consequently, several authors have developed, examined, and reviewed nonlinear rotor models [7-9].

In Machado et al. [8], journal bearings were subjected to several operating conditions to

evaluate different nonlinear behaviors such as the structural damping effect, the gyroscopic effect, journal eccentricity and external excitation force. The differences between linear and nonlinear models could be seen through simulation of the journal orbits inside the bearings, which was then supported by experimental results. It was determined that external excitation had the largest nonlinear impact on hydrodynamic forces. As the unbalance mass increased, the results from linear and nonlinear techniques diverged, showing that the linear model was inadequate for system representation under these circumstances. Moreover, in Viana et al. [7], with the system running under high loading conditions, the limits of linear approximation of the hydrodynamic forces present in lobed hydrodynamic bearings was examined. Several simulations with varying preload parameters and rotating speed were conducted. For both linear and nonlinear models, the responses of the system were compared in the time domain and the frequency domain. The results showed that the trilobed bearings were more sensitive to nonlinearities, even in cases of low vibration amplitudes, whereas elliptical bearings were only sensitive in conditions with high vibration amplitudes.

Several researchers have studied the behavior of worn bearings utilized in rotating machines. Dufrane et al. [2] examined the wear present in steam turbine bearings by taking measurements at predetermined time frames to determine the nature and extent of wear. For a more in-depth examination of the effect of wear on journal bearing, two wear geometry models were developed and utilized. Machado and Cavalca [10] developed a mathematical representation for the static analysis of journal bearing by utilizing the Reynolds equation. They computed the pressure distribution in the bearing and examined the performance of dissimilar geometries in severe conditions, high speeds, and high-applied load. Papanikolaou et al. [11] investigated the effect of wear of a short journal bearing on the dynamic stiffness and damping coefficients. Machado and Cavalca [12] introduced a mathematical model to represent geometric discontinuities in journal bearing. They further presented a mathematical model that described the wear present in journal bearings and the effect of the wear on the dynamic response of the rotor-bearing system in frequency domain. Jamil et al. [13] investigated the impact of wear in journal bearings on the dynamic behavior of rotor bearing system using linearized dynamic stiffness and damping coefficients of worn journal bearing. Turaga et al. [14] utilized the linearized perturbation method and the nonlinear transient analysis method to examine the sub-synchronous whirl stability limit of a rigid rotor supported on two symmetrical finite journal bearings. They demonstrated that the results from the linear analysis are predicted with reasonably accuracy for steady-state eccentricity ratio less than 0.7. However, the nonlinear analysis revealed noticeably higher stability limits at higher steady-state eccentricity ratio, especially for lower length / diameter ratios of the bearings.

This study differs from previous studies on rotor responses in nonlinear journal bearings in the sense that most previous studies have focused on comparing only linear and nonlinear responses in non-worn journal bearings [7, 8]. The present study aims to make a comparison between the linear and nonlinear responses of rotor mounted in worn journal bearings to investigate the effect of bearing wear severity on the dynamic behavior of the rotor-bearing system. This study also differs from the work of Jamil et al. [13], which utilized linearized dynamic coefficients, a linear approach, to predict the response of the rotor, whereas the current work uses nonlinear bearing forces, a nonlinear approach. A comparison on the rotor response produced by using the linearized dynamic coefficients and the nonlinear bearing forces are made to explore the limitations of using linearized dynamic coefficients to model wear in journal bearings. The necessity to carry out this work stems from the fact that as wear depth increases in journal bearings, the oil-film clearances also increase, which in turn causes the bearings to behave nonlinearly.

## 2. Mathematical treatment

This section focuses on the derivation of nonlinear bearing forces. The derivation of linearized dynamic stiffness and damping coefficients of the bearing can be referred to the work of Papanikolaou et al. [11] and Jamil et al. [13].

### 2.1 Wear model

The wear model used in this paper is the model proposed by Dufrane et al. [2], and it is shown in Fig. 1 [11].

$O_b$ is the bearing center; $O_j$ is the journal center; $e$ is the eccentricity, defined as the distance between the bearing center and the journal center (m); $h_0$ is the fluid film thickness in the non-worn region (m); $h_w$ is the fluid film thickness in the worn region (m); $\gamma$ is the circumferential coordinate, measured counter-clockwise from the negative *X*-axis (rad); $\theta$ is the circumferential coordinate (rad); $\varphi_0$ is the attitude angle at the static equilibrium position (rad); $\theta_s$ is the circumferential coordinate of the starting point of the worn region (rad); $\theta_f$ is the circumferential coordinate of the final point of the worn region (rad); $\omega$ is the angular speed of the rotor (rad/s); $d_0$ is the maximum wear depth (m); *W* is the bearing load (N); *X* and *Y* are coordinates of the journal center.

The region of positive pressure in the state of worn journal bearing can be divided into three sub regions. Following an anticlockwise direction, the 1st sub region (1st yellow shading) is the 1st non-worn region $(0 \le \theta \le \theta_s)$, the 2nd sub region (green shading) is the worn region ($\theta_s \le \theta \le \theta_f$) and the 3rd sub region (2nd yellow shading) is the 2nd non-worn region ($\theta_f \le \theta \le \pi$). The starting and final angles of the region where the wear takes place (refer to Fig. 1) are given by [13]:

$$cos(\theta + \varphi_0) = \frac{d_0}{C} - 1 = \delta - 1 \tag{1}$$

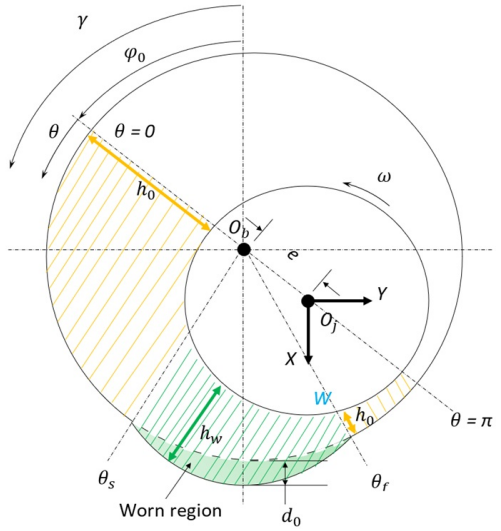


Fig. 1. Geometry of a worn journal bearing indicating the worn region within the circumferential extent of the oil-film for a specific static equilibrium position (adapted from Ref. [11]). Starting and final points of the worn region are respectively denoted by the circumferential coordinate $\theta_s$ and $\theta_f$.

where $\delta = \frac{d_0}{C}$; $\delta$ is the wear depth parameter.

$\theta_s$ and $\theta_f$ are represented by the following equations [13]:

$$\theta_s = \pi - \varphi_0 - \arccos(1-\delta) \tag{2}$$

$$\theta_f = \pi - \varphi_0 + \arccos(1-\delta). \tag{3}$$

The derivation of equations for fluid film thickness in non-worn and worn bearing regions has been presented in Ref. [13].

## 2.2 Solution to nonlinear bearing forces

The fluid film pressure is obtained by solving the Reynolds equation for infinitely short bearing. For convenience purposes, polar coordinates are employed instead of Cartesian coordinates to solve the Reynolds equation.

The following assumptions are made in the determination of the pressure distribution in the bearing: (i) short journal bearing, (ii) laminar fluid flow, (iii) iso-viscous fluid, (iv) incompressible fluid, and (v) $\pi$-film cavitation model [13].

By integrating the Reynolds equation with respect to the axial coordinate, *Z*, the pressure distribution for the non-worn and worn regions are obtained [13].

The pressure distribution in the non-worn region, *P*, is expressed by Eq. (4) below.

$$P(\theta,Z,t) = \frac{6\mu}{h^3}\left(\frac{\partial h}{\partial t} + \frac{\Omega}{2}\frac{\partial h}{\partial \theta}\right)\left(Z^2 - \frac{L^2}{4}\right) \tag{4}$$

where *L* is the journal bearing length (m), *Z* is the axial distance in the direction of Z-axis and $h$ is the fluid film thickness in the non-worn region of the journal bearing.

The pressure distribution in the worn region, $P_w$, is expressed by Eq. (5).

$$P_w(\theta,Z,t) = \frac{6\mu}{h^3}\left(\frac{\partial h_w}{\partial t} + \frac{\Omega}{2}\frac{\partial h_w}{\partial \theta}\right)\left(Z^2 - \frac{L^2}{4}\right) \tag{5}$$

where $P_w$ is the pressure in the worn region of the journal bearing and $h_w$ is the fluid film thickness in the worn region of the journal bearing.

The radial and tangential bearing forces, presented in Eq. (6), are obtained by integrating the pressure distribution given in Eqs. (4) and (5) along the axial coordinate, *Z*.

$$\begin{aligned}
F_r = -\frac{\mu R L^3}{c^2}\Bigg[ & \int_{\theta_1}^{\theta_s} \frac{(\dot{\varphi}-0.5\omega)\varepsilon\sin\theta\cos\theta + \dot{\varepsilon}\cos^2\theta + \varepsilon\dot{\varphi}\sin\theta\cos\theta}{(1+\varepsilon\cos\theta)^3} d\theta \\
& + \int_{\theta_s}^{\theta_f} \frac{(\dot{\varphi}-0.5\omega)\left(\varepsilon\sin\theta\cos\theta + \sin(\theta+\varphi)\cos\theta\right) + \dot{\varepsilon}\cos^2\theta + \varepsilon\dot{\varphi}\sin\theta\cos\theta}{(\delta+\varepsilon\cos\theta-\cos(\theta+\varphi))^3} d\theta \\
& + \int_{\theta_f}^{\pi} \frac{(\dot{\varphi}-0.5\omega)\varepsilon\sin\theta\cos\theta + \dot{\varepsilon}\cos^2\theta + \varepsilon\dot{\varphi}\sin\theta\cos\theta}{(1+\varepsilon\cos\theta)^3} d\theta \Bigg] \\
F_t = -\frac{\mu R L^3}{c^2}\Bigg[ & \int_{\theta_1}^{\theta_s} \frac{(\dot{\varphi}-0.5\omega)\varepsilon\sin^2\theta + \dot{\varepsilon}\sin\theta\cos\theta + \varepsilon\dot{\varphi}\sin^2\theta}{(1+\varepsilon\cos\theta)^3} d\theta \\
& + \int_{\theta_s}^{\theta_f} \frac{(\dot{\varphi}-0.5\omega)\left(\varepsilon\sin^2\theta + \sin(\theta+\varphi)\sin\theta\right) + \dot{\varepsilon}\sin\theta\cos\theta + \varepsilon\dot{\varphi}\sin^2\theta}{(\delta+\varepsilon\cos\theta-\cos(\theta+\varphi))^3} d\theta \\
& + \int_{\theta_f}^{\pi} \frac{(\dot{\varphi}-0.5\omega)\varepsilon\sin^2\theta + \dot{\varepsilon}\sin\theta\cos\theta + \varepsilon\dot{\varphi}\sin^2\theta}{(1+\varepsilon\cos\theta)^3} d\theta \Bigg]
\end{aligned} \tag{6}$$

where $\theta_1 = \left(-\frac{\dot{\varepsilon}}{\varepsilon(\dot{\varphi}-0.5\omega)}\right)$.

The forces in the radial and tangential directions, given in Eq. (6), can be transformed into forces in the Cartesian coordinates (*X*- and *Y*-directions) using the following equations [15].

$$\begin{Bmatrix} F_x \\ F_y \end{Bmatrix} = \begin{Bmatrix} F_r\cos\varphi - F_t\sin\varphi \\ F_r\sin\varphi + F_t\cos\varphi \end{Bmatrix}. \tag{7}$$

## 2.3 Equations of motion of a rigid rotor in journal bearings

A rigid rotor model is considered in this work, and only motion in the *X*- and *Y*-directions is considered. The axial motion

of the rotor is neglected. Let the rotor mass be 2*M* and the journal center amplitudes $\bar{x}$ and $\bar{y}$.

The equations of motion for the nonlinear model are given by:

$$M\frac{d^2\bar{x}}{dt^2} = F_x + MU\omega^2\cos\omega t + W$$
$$M\frac{d^2y}{dt^2} = F_y + MU\omega^2\sin\omega t\,. \tag{8}$$

The equations are made dimensionless following the work by Lund et al. [16], and they are expressed as follows:

$$m\ddot{x} = f_x + mu\cos\tau + \sigma^{-1}$$
$$m\ddot{y} = f_y + mu\sin\tau\,. \tag{9}$$

## 3. Numerical simulation

The wear model proposed by Dufrane et al. [2], as shown in Fig. 1, was used in the present work. The bearing was modelled using the short journal bearing ($L/D \leq 0.5$) approximation, where *L* is the length of the bearing and *D* is the diameter of the journal. Half Sommerfeld (Gumbel's) boundary condition was used to model the extent of the oil-film. The numerical simulation to examine the effect of wear on the nonlinear and linear vibration responses of the rotor was undertaken for 3 different operating load regimes, namely low loaded operating regime ($0.1 \leq \varepsilon_0 \leq 0.2$), moderately loaded operating regime ($0.3 \leq \varepsilon_0 \leq 0.5$) and highly loaded operating regime ($0.6 \leq \varepsilon_0 \leq 0.75$) [17]. $\varepsilon_0$ is the steady-state eccentricity ratio, which is the ratio of the eccentricity, defined as the distance between the bearing center and the journal center, to the radial clearance of the bearing under static equilibrium condition. The unbalance parameter *U* was set at 0.05. The dimensionless journal mass *m* was set at 0.993 for low loaded operating regime, 4.717 for moderately loaded operating regime and 28.599 for highly loaded operating regime. The wear depth parameter ratio $\delta$ was varied from 0 to 0.1 and the results are presented for $\delta$ increments of 0.02.

The journal bearing forces given in Eq. (6) were solved using the Simpson's 1/3 rule in MATLAB. The non-linear equations of motion, presented in Eq. (9), were solved using MATLAB's Runge-Kutta (4, 5) algorithm. The linear equations of motion, on the other hand, were solved using the MATLAB's linear solver. The numerical results were presented as rotor whirl orbits, average shaft centreline plots, and power spectrum.

## 4. Results and discussion

This section focuses on the results obtained from the numerical simulation. The results are discussed to examine the differences between the nonlinear and linear responses in worn journal bearing, and the effect of wear on nonlinear responses in worn journal bearing.

### 4.1 Nonlinear and linear responses in worn journal bearing

Fig. 2 show the nonlinear and linear whirl orbit plots of the rotor response in the lightly loaded operating regime, moderately loaded operating regime, and highly loaded operating regime for $\delta = 0$ and $\delta = 0.1$, respectively.

It is observed that in Fig. 2(a), when $\delta$ = 0, the shaft centreline of the nonlinear orbit coincides with the shaft centreline of the linear orbit. However, as $\delta$ increases, as in Fig. 2(b), the shaft centerline of the nonlinear orbit shifts further away from the shaft centerline of the linear orbit with a significant shift in the *X*-direction by 71.7 % for the lightly loaded operating regime and 39.1 % for the moderately loaded operating regime. As for the highly loaded operating regime, a significant shift in the *Y*-direction by 156.8 % is noticed. Also, the size of the

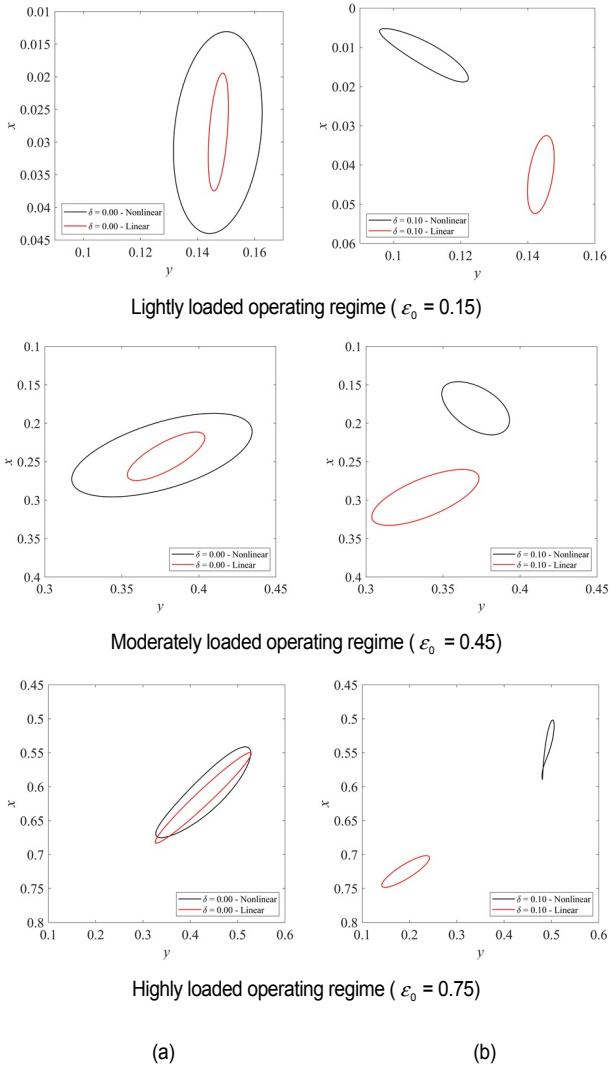


Lightly loaded operating regime ( $\varepsilon_0$ = 0.15)

Moderately loaded operating regime ( $\varepsilon_0$ = 0.45)

Highly loaded operating regime ( $\varepsilon_0$ = 0.75)

(a) (b)

Fig. 2. Nonlinear and linear whirl orbit plots of the rotor response in the lightly loaded operating regime ( $\varepsilon_0$ = 0.15), moderately loaded operating regime ( $\varepsilon_0$ = 0.45), and highly loaded operating regime ( $\varepsilon_0$ = 0.75 ) for (a) $\delta$ = 0; (b) $\delta$ = 0.1.

nonlinear orbit is larger than the linear orbit when $\delta$ = 0.

Moreover, when $\delta$ = 0, in lightly loaded operating regime, the orbital shape and orientation for nonlinear and linear response is similar. The nonlinear orbit remains elliptical as $\delta$ is increased from 0 to 0.1. As for moderately loaded operating regime, when $\delta$ = 0, the nonlinear orbital shape is elliptical, and the orientation is almost like the linear response. The nonlinear orbital shape becomes less elliptical with increasing $\delta$. While highly loaded operating regime shows a nonlinear orbital shape and orientation that follows much closely to the linear response when $\delta$ = 0. The nonlinear orbital shape becomes less elliptical and more deformed with increasing $\delta$. In all these figures, it is observed that the nonlinear orbital shape and the orientation does not follow the linear response as $\delta$ is increased from 0 to 0.1.

### 4.2 Effect of wear on nonlinear responses in worn journal bearing

Fig. 3(a) shows the nonlinear whirl orbits in the lightly loaded operating regime, moderately loaded operating regime, and highly loaded operating regime respectively. It is observed that the size of the nonlinear orbit reduces and a significant shift in nonlinear orbit orientation in the anticlockwise direction is apparent when $\delta$ is increased from 0 to 0.1. In addition, in the highly loaded operating regime, it is observed that the nonlinear orbit deforms considerably as $\delta$ is increased from 0 to 0.1. As a result, at $\delta = 0.1$, a super-synchronous response is seen.

Furthermore, Fig. 3(b) shows the nonlinear shaft centerline in the lightly loaded operating regime, moderately loaded operating regime, and highly loaded operating regime respectively. As $\delta$ is increased from 0 to 0.1, this figure shows that the nonlinear shaft centerline moves closer towards the center of the unit circle. In Fig. 3(b), in the lightly loaded operating regime, there seems to be a smaller displacement in the *Y*-direction (horizontal axis) by 26 % than the displacement in the *X*-direction (vertical axis) by 58 %. Whereas in moderately loaded operating regime, there seems to be a smaller displacement in the *Y*-direction (horizontal axis) by 1.3 % than the displacement in the *X*-direction (vertical axis) by 25 %. However, in contrast to lightly loaded operating regime and moderately loaded operating regime, there seems to be a larger displacement in the *Y*-direction (horizontal axis) by 15 % than the displacement in the *X*-direction (vertical axis) by 10 % as observed in the highly loaded operating regime.

Fig. 4 shows the power spectrum of the nonlinear rotor response in the highly loaded operating regime for $\delta = 0.1$. Two peaks are observed at 1 X RPM (synchronous) and 2 X RPM (super-synchronous). Nonlinearity in the rotor response is evidenced by the appearance of higher order harmonic component. The nonlinear orbit's size and shape is influenced by the additional harmonic component [7], which can be clearly observed in highly loaded operating regime as shown in Fig. 2(b).

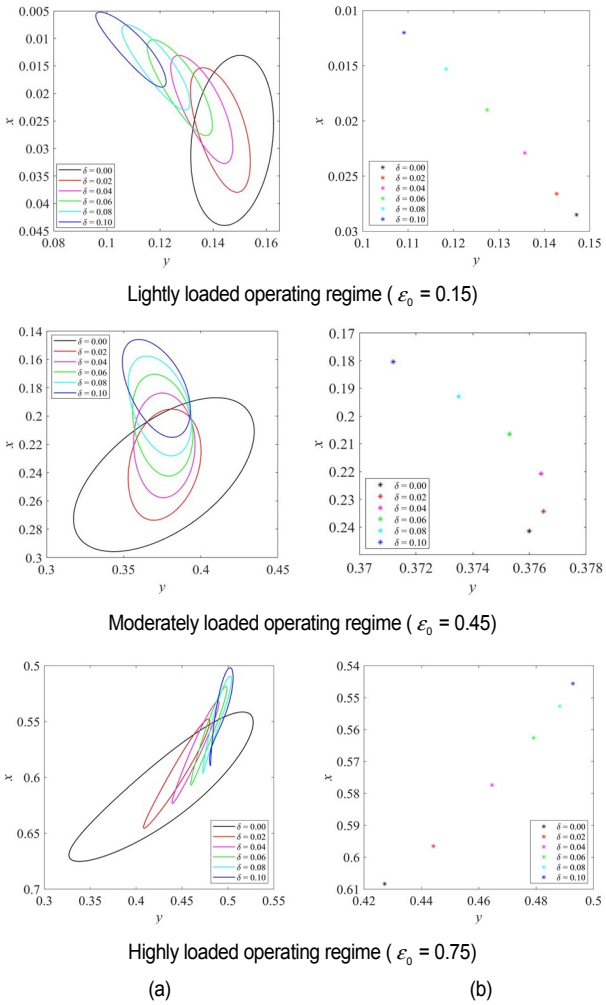


Fig. 3. (a) Nonlinear rotor whirl orbits; (b) nonlinear shaft centerline in the lightly loaded operating regime ( $\varepsilon_0$ = 0.15), moderately loaded operating regime ( $\varepsilon_0$ = 0.45), and highly loaded operating regime ( $\varepsilon_0$ = 0.75) for $\delta$ = 0.0 to 0.1 (in intervals of 0.02).

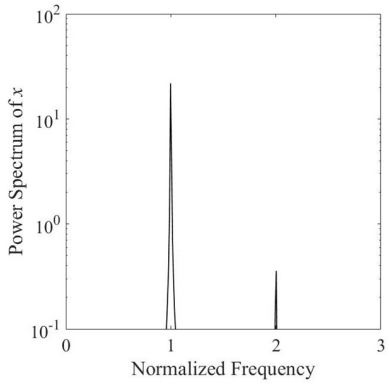


Fig. 4. Power spectrum of the nonlinear rotor response in the highly loaded operating regime ( $\varepsilon_0$ = 0.75) for $\delta$ = 0.1, *m* = 28.599 & *U* = 0.05.

## 5. Conclusions

The effect of bearing wear on the linear and nonlinear re-

sponses of a rigid rotor was investigated for 3 different operating regimes, namely low loaded operating regime, moderately loaded operating regime and highly loaded operating regime. The wear depth parameter, $\delta$, was varied from 0 to 0.1, in increments of 0.02. Numerical results showed that when $\delta$ = 0, the vibration amplitude for the nonlinear response was larger than the linear response, and the center of the nonlinear orbit coincided with the center of the linear orbit for all three operating regimes. When $\delta$ was increased, however, the center of the nonlinear orbit shifts away from the center of the linear orbit for all three operating regimes. Synchronous response was observed for both linear and nonlinear vibration responses except when the rotor operates at $\varepsilon_0$ = 0.75 and $\delta$ = 0.1, where a super-synchronous response (2X RPM) was observed for the nonlinear response. The outcome of the present work indicated that when wear occurs in journal bearings, computation of the vibration response of the rotor using the linearized dynamic coefficients of these bearings may considerably differ from that using the nonlinear bearing forces.

## Acknowledgements

This work was supported by Tenaga Nasional Berhad (TNB) and UNITEN through the BOLD 2023 Research Grant under the project code of J510050949. The first author would also like to express his sincere gratitude to Universiti Tenaga Nasional for awarding him the UNITEN-YCU Postgraduate Scholarship to support his studies.

## Nomenclature

$c$ : Radial clearance, m
$D$ : Journal diameter, m
$d_0$ : Wear depth, m
$e$ : Eccentricity between journal center and bearing center, m
$F_x, F_y$ : $X$- and $Y$-component of fluid film journal bearing force, N
$f_x, f_y$ : Non-dimensional $X$- and $Y$-component of fluid film journal bearing force
$F_r, F_t$ : Radial and tangential component of fluid film journal bearing force, N
$h$ : Fluid film thickness at non-worn region, m
$h_0$ : Initial fluid film thickness at non-worn region, m
$h_w$ : Fluid film thickness at worn region, m
$L$ : Bearing length, m
$M$ : Rotor mass, m
$m$ : Non-dimensional rotor mass
$O_b$ : Bearing center
$O_j$ : Journal center
$P$ : Fluid film oil pressure of non-worn region, Pa
$P_w$ : Fluid film oil pressure of worn region, Pa
$R$ : Journal radius, m
$t$ : Time, s
$U$ : Unbalance force, N
$u$ : Non-dimensional unbalance force
$W$ : Bearing load, N
$X, Y$ : Coordinates of the journal center
$x, y$ : Coordinates of the journal center, normalized with respect to $c$
$\bar{x}, \bar{y}$ : Journal center amplitudes
$Z$ : Axial distance in the direction of $Z$-axis, m
$\gamma$ : Circumferential coordinate from $X$-axis, rad
$\delta$ : Wear depth parameter ratio
$\varepsilon$ : Eccentricity ratio
$\varepsilon_0$ : Steady-state eccentricity ratio
$\theta$ : Circumferential coordinate, rad
$\theta_s$ : Circumferential coordinate of the starting point of the worn region, rad
$\theta_f$ : Circumferential coordinate of the final point of the worn region, rad
$\mu$ : Viscosity, Pa s
$\varphi$ : Attitude angle, rad
$\varphi_0$ : Attitude angle at static equilibrium position, rad
$\omega$ : Angular speed of the rotor, rad/s
$\sigma$ : Modified Sommerfeld number
$\tau$ : Non-dimensional time

## References

[1] D. Childs, Turbomachinery rotordynamics phenomena, *Modeling and Analysis*, Wiley, USA (1993).
[2] K. F. Dufrane, J. W. Kannel and T. H. McCloskey, Wear of steam turbine journal bearings at low operating speeds, *Journal of Lubrication Technology*, 105 (3) (1983) 313-317.
[3] F. K. Choy, M. J. Braun and Y. Hu, Nonlinear effects in a plain journal bearing: part 1 - analytical study, *ASME Journal of Tribology*, 113 (1991) 555-561.
[4] K. Gertzos, P. Nikolakopoulos, A. Chasalevris and C. Papadopoulos, Wear identification in rotor-bearing systems by measurements of dynamic bearing characteristics, *Computers & Structures*, 89 (1-2) (2011) 55-66.
[5] J. W. Lund and K. K. Thomsen, A calculation method and data for the dynamic coefficients of oil-lubricated journal bearings, *Des Eng Conf C* (*Topics in Fluid Film Bearing and Rotor Bearing System Design and Optimization)*, USA (1978) 1-28.
[6] J. W. Lund, Review of the concept of dynamic coefficients for fluid film journal bearings, *ASME Journal of Tribology*, 109 (1987) 37-41.
[7] C. A. A. Viana, D. S. Alves and T. H. Machado, Linear and nonlinear performance analysis of hydrodynamic journal bearings with different geometries, *Applied Sciences*, 12 (7) (2022) 3215.
[8] T. H. Machado, D. S. Alves and K. L. Cavalca, Discussion about nonlinear boundaries for hydrodynamic forces in journal bearing, *Nonlinear Dynamics*, 92 (4) (2018) 2005-2022.
[9] S. Kim, D. Shin and A. B. Palazzolo, A review of journal bearing induced nonlinear rotordynamics vibrations, *ASME Journal of Tribology*, 143 (11) (2021) 111802.
[10] T. H. Machado and K. L. Cavalca, Evaluation of hydrodynamic bearings with geometric discontinuities, *Proceedings of the 21st Brazilian Congress of Mechanical Engineering*, Natal,

Brazil (2011).
[11] M. G. Papanikolaou, M. G. Farmakopoulos and C. A. Papadopoulos, Alternation of the dynamic coefficients of short journal bearings due to wear, *International Journal of Structural Integrity*, 6 (5) (2015) 649-664.
[12] T. H. Machado and K. L. Cavalca, Geometric discontinuities identification in hydrodynamic bearings, *Proceedings of the 9th IFToMM International Conference on Rotor Dynamics, Mechanism and Machine Science*, Springer, Chem, Switzerland (2015).
[13] A. N. Jamil, A. A. H. Ali and T. Mohammad, Study the dynamic behavior of rotor supported on a worn-journal bearings, *Engineering*, 21 (12) (2015) 1-18.
[14] R. Turaga, A. S. Sekhar and B. C. Majumdar, Comparison between linear and nonlinear transient analysis techniques to find the stability of a rigid rotor, *ASME Journal of Tribology*, 121 (1999) 198-201.
[15] L. San Andrés, Hydrodynamic fluid film bearings and their effect on the stability of rotating machinery, *Design and Analysis of High Speed Pumps; Educational Notes RTO-ENAVT-143*, NATO, France (2006) 10-1-10-36.
[16] J. W. Lund and E. Saibel, Oil whip whirl orbits of a rotor in sleeve bearings, *ASME Journal of Engineering for Industry*, 89 (4) (1967) 813-823.
[17] A. Zakaria and J. I. Inayat-Hussain, Bifurcation analysis of rigid rotor supported by nonlinear journal bearing, *2nd International Conference on Mechanical, Automotive and Aerospace Engineering (ICMAAE 2013)*, Kuala Lumpur, Malaysia (2013).

**Logamurthi Raja Moorthi** is a Mechanical Engineer in Tenaga Nasional Berhad, Malaysia. He is currently pursuing his Masters of Mechanical Engineering at Universiti Tenaga Nasional (UNITEN), Malaysia under the Yayasan Chancellor UNITEN scholarship fund. His field of study is in mechanical vibrations.

**Jawaid I. Inayat-Hussain** is an Associate Professor of the College of Engineering, Universiti Tenaga Nasional, Malaysia. He received his Ph.D. in Mechanical Engineering from Kobe University, Japan. His research interests are in the areas of rotordynamics, vibration and noise control, and machinery condition monitoring.

**Azrul Abidin Zakaria** is a Senior Lecturer of the College of Engineering, Universiti Tenaga Nasional, Malaysia. He received his Ph.D. in Mechanical Engineering from University of Southampton, United Kingdom. His research interests include mechanical vibrations, engineering graphics, computer aided engineering, and machine design.